

*Electronic Supporting Information
for*

**Electron-rich linear triplatinum complexes stabilized by spinning
tetraphosphine, tris(diphenylphosphinomethyl)phosphine**

**Tomoaki Tanase,* Kanako Koike, Miho Uegaki, Satoko Hatada, Kanako Nakamae,
Bunsho Kure, Yasuyuki Ura and Takayuki Nakajima***

*Department of Chemistry, Faculty of Science, Nara Women's University,
Kitauoya-nishi-machi, Nara 630-8506, Japan.*

Fax: +81 742 203847; Tel: +81 742 203399; E-mail: tanase@cc.nara-wu.ac.jp

Table S1. Crystallographic and experimental data of **3**·2CH₂Cl₂ and **4**·2CH₂Cl₂.

Table S2. Selected bond lengths and angles of **3** and **4**.

Figure S1. ESI–TOF mass spectra of **3** in CH₃OH.

Figure S2. ESI–TOF mass spectra of **4** in CH₃OH.

Figure S3. ³¹P{¹H} NMR spectra of **4** at (a) 60 °C, (b) 20 °C, and (c) –30 °C in CD₃CN and the assignments.

Figure S4. Variable temperature UV–vis absorption spectra of **3** in CD₃CN.

Figure S5. (a) Representative MO diagrams from the DFT calculations on

[Pt₃(μ–tdpmp)₂(^tBuNC)₂]²⁺ (**4**) by B3LYP methods with lanl2dz and PCM (CH₂Cl₂), and (b) the results of TD–DFT calculations.

Figure S6. (a) Representative MO diagrams from the DFT calculations on

[Pt₃(μ–dpmp)₂(^tBuNC)₂]²⁺ (**2**) by B3LYP methods with lanl2dz and PCM (CH₂Cl₂), and (b) the results of TD–DFT calculations.

Table S1. Crystallographic and experimental data of **3·2CH₂Cl₂** and **4·2CH₂Cl₂**.

Compound	3·2CH₂Cl₂	4·2CH₂Cl₂
formula	C ₉₈ H ₉₄ Cl ₄ N ₂ F ₁₂ P ₁₀ Pt ₃	C ₉₀ H ₉₄ Cl ₄ N ₂ F ₁₂ P ₁₀ Pt ₃
formula wt	2564.63	2468.55
cryst. syst	triclinic	monoclinic
space group	<i>P</i> -1	<i>P</i> 2 ₁ /n
<i>a</i> , Å	13.328(4)	11.5968(9)
<i>b</i> , Å	14.042(5)	21.9132(13)
<i>c</i> , Å	15.350(5)	18.8936(15)
α, deg	107.847(2)	
β, deg	114.560(5)	97.800(4)
γ, deg	94.641(3)	
<i>V</i> , Å ³	2414.0(14)	4756.9(6)
<i>Z</i>	1	2
temp, °C	-120	-120
<i>D</i> _{calcd} , g cm ⁻¹	1.764	1.723
μ, mm ⁻¹ (Mo Kα)	4.666	4.732
2θ range, deg	6–55	6–55
<i>R</i> _{int}	0.048	0.044
no. of reflns collected	19548	44367
no. of unique reflns	10465	10690
no. of obsd reflns	7783	6815
(<i>I</i> > 2σ(<i>I</i>))		
no. of variables	584	548
<i>R</i> 1 ^a	0.060	0.037
<i>wR</i> 2 ^b	0.145	0.109
<i>GOF</i>	1.095	0.994

^a *R*1 = Σ | |*F*_o| - |*F*_c| | / Σ |*F*_o| (for obsd. refs with *I* > 2σ(*I*)). ^b *wR*2 = [Σ*w*(*F*_o² - *F*_c²)² / Σ*w*(*F*_o²)²]^{1/2} (for all refs).

Table S2. Selected bond lengths (\AA) and angles ($^\circ$) of **3** and **4**.^a

	3	4
Pt1–Pt2	2.7779(2)	2.72840(16)
Pt1–P1	2.342(2)	2.3282(11)
Pt1–P2	2.476(2)	2.3529(12)
Pt1–P3*	2.321(2)	2.3105(11)
Pt1–C1	1.991(8)	1.970(5)
Pt2–P4	2.237(2)	2.2378(11)
C1–N1	1.183(12)	1.050(7)
Pt1–Pt2–Pt1*	180	180
Pt2–Pt1–P1	78.05(4)	82.13(2)
Pt2–Pt1–P2	92.37(4)	86.07(2)
Pt2–Pt1–P3*	84.25(4)	90.24(2)
Pt2–Pt1–C1	165.1(2)	178.79(14)
P1–Pt1–P2	91.98(9)	101.17(4)
P1–Pt1–P3*	141.78(8)	134.00(4)
P2–Pt1–P3*	122.66(8)	123.59(3)
P1–Pt1–C1	98.8(2)	96.76(13)
P2–Pt1–C1	102.4(3)	94.64(16)
P3*–Pt1–C1	89.7(2)	90.20(13)
Pt1–Pt2–P4	83.38(4)	83.23(2)
Pt1–Pt2–P4*	96.68(4)	96.77(2)

^a The atomic numbering schemes are shown in Figure 1.

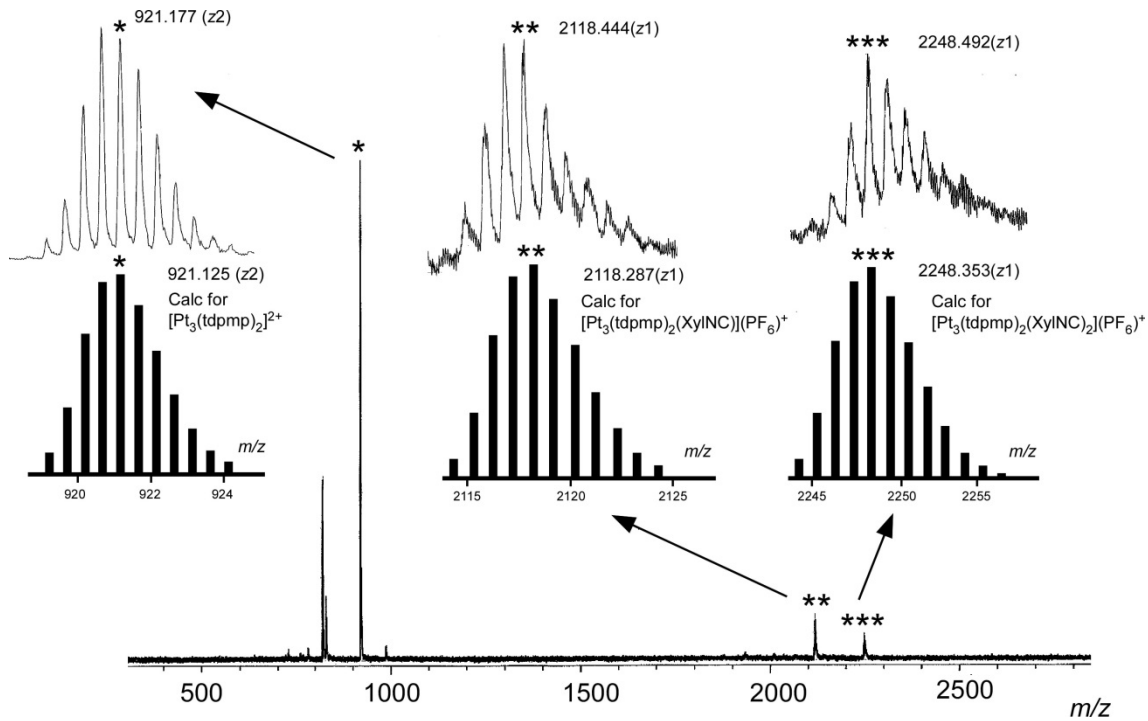
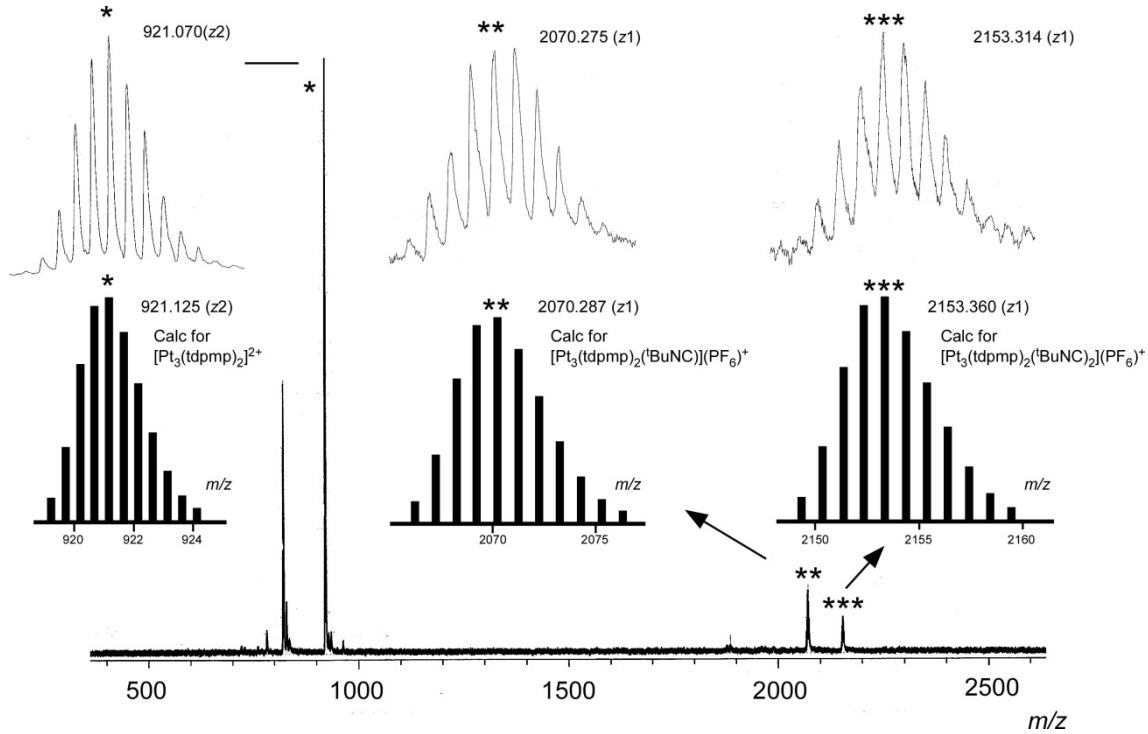
Figure S1. ESI–TOF mass spectra of **3** in CH₃OH.**Figure S2.** ESI–TOF mass spectra of **4** in CH₃OH.

Figure S3. $^{31}\text{P}\{\text{H}\}$ NMR spectra of **4** at (a) 60 °C, (b) 20 °C, and (c) -30 °C in CD_3CN and the assignments.

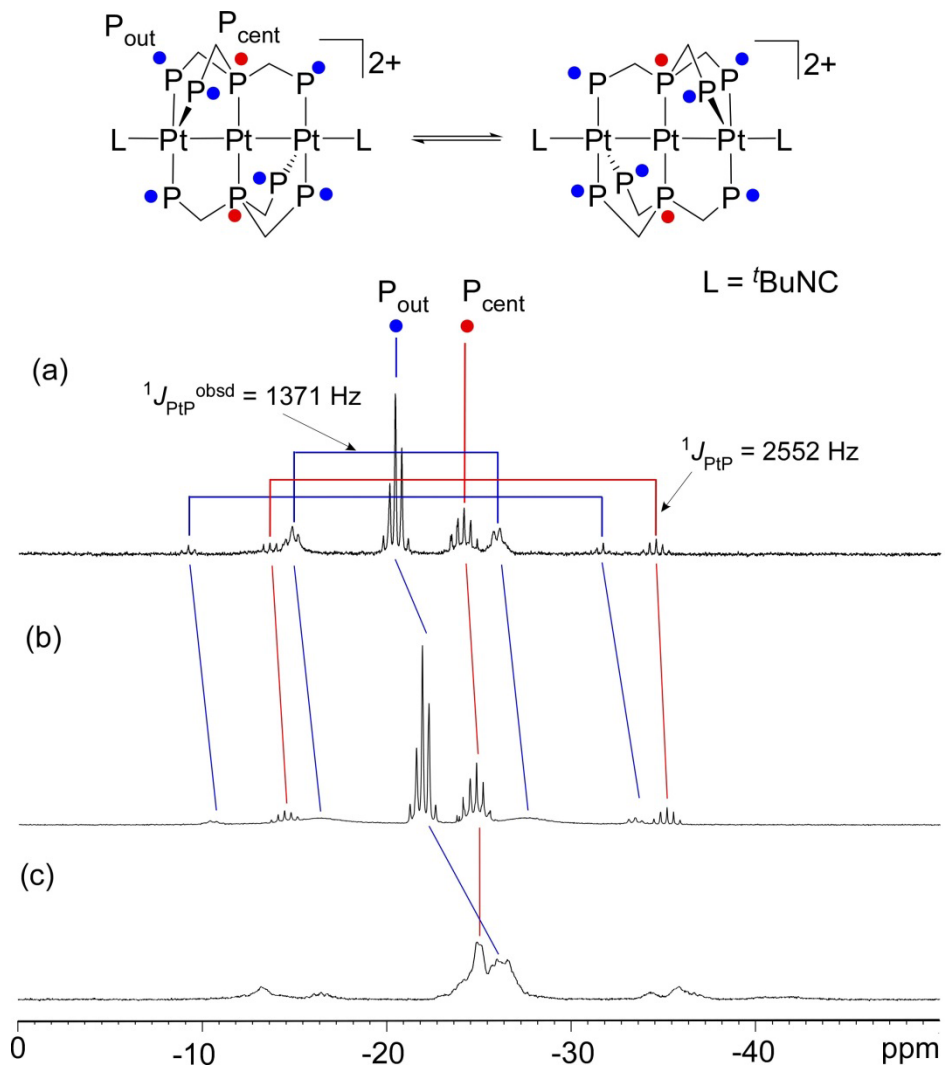


Figure S4. Variable temperature UV-vis absorption spectra of **3** in CD₃CN; (a) from 20 °C to -30 °C, and (b) from 20 °C to 60 °C.

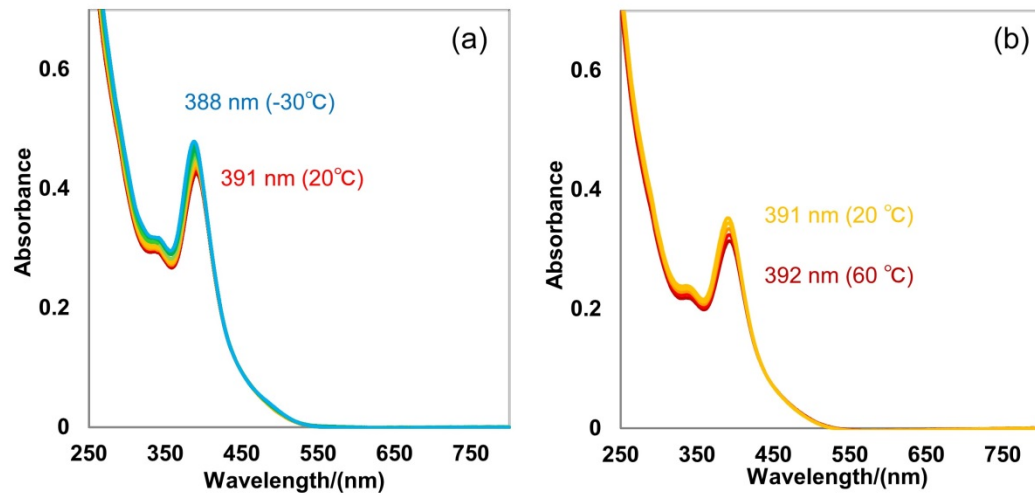
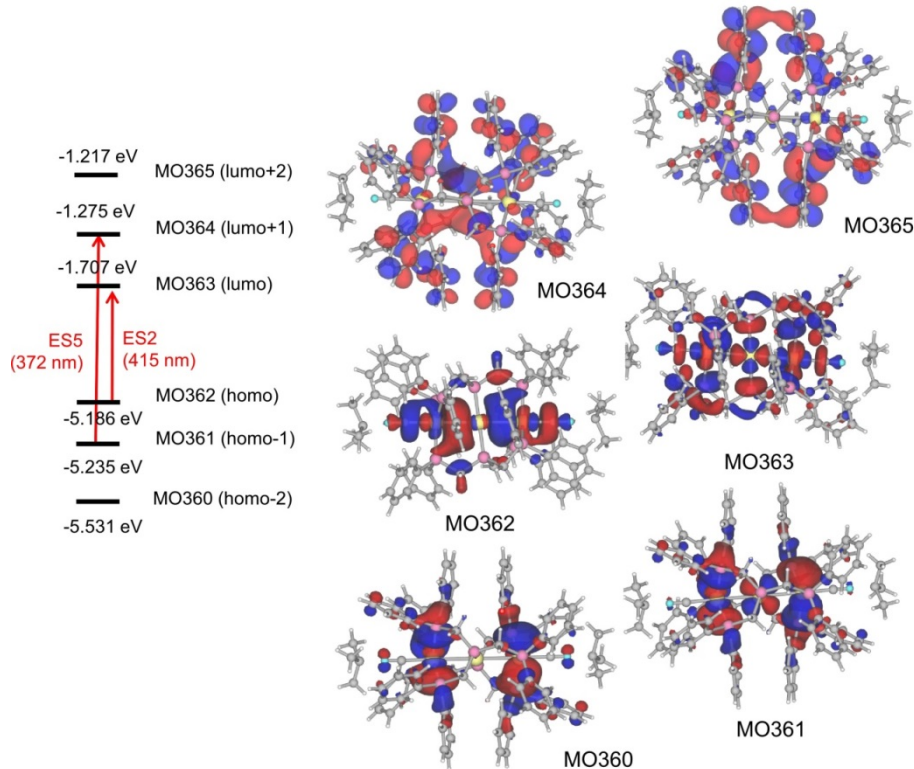


Figure S5. (a) Representative MO diagrams for the DFT calculations on $[\text{Pt}_3(\mu\text{-tdpmp})_2(\text{BuNC})_2]^{2+}$ (**4**) by B3LYP methods with lanl2dz and PCM (CH_2Cl_2), and (b) the results of TD-DFT calculations.

(a)

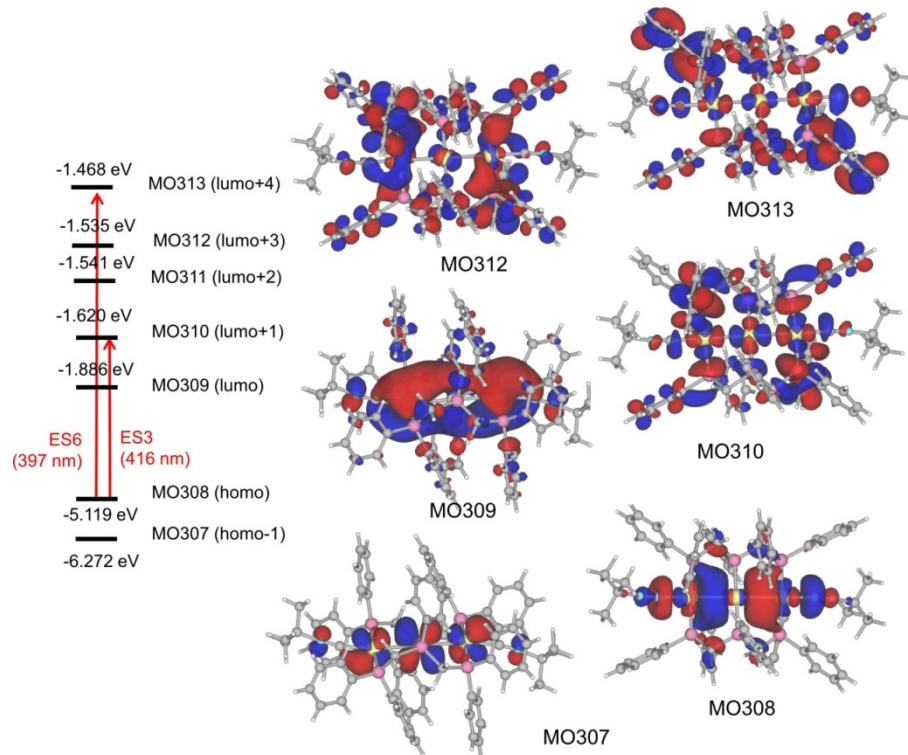


(b)

	TD-DFT data				obsd (CH_2Cl_2)
Excited States	energy/eV	λ/nm	f	transitions	λ/nm
E1	2.682	462	0.0001	$361 \rightarrow 363$ (0.67)	
E2	2.986	415	0.4943	$361 \rightarrow 364$ (0.11) $362 \rightarrow 363$ (0.64)	392
E3	3.044	407	0.036	$360 \rightarrow 363$ (0.67)	
E4	3.276	379	0.0001	$362 \rightarrow 364$ (0.68)	
E5	3.333	372	0.0926	$361 \rightarrow 364$ (0.66) $361 \rightarrow 366$ (-0.11)	342
E6	3.428	362	0.0244	$362 \rightarrow 365$ (0.67)	
E7	3.433	361	0.0001	$361 \rightarrow 365$ (0.65)	
E8	3.459	358	0.0001	$362 \rightarrow 366$ (0.67)	

Figure S6. (a) Representative MO diagrams for the DFT calculations on $[\text{Pt}_3(\mu-\text{dpmp})_2(^t\text{BuNC})_2]^{2+}$ (**2**) by B3LYP methods with lanl2dz and PCM (CH_2Cl_2), and (b) the results of TD-DFT calculations.

(a)



(b)

	TD-DFT data				obsd (CH_2Cl_2)
Excited States	energy/eV	λ/nm	f	transitions	λ/nm
E1	2.491	498	0.0001	308→309 (0.69)	496
E2	2.916	425	0.0153	308→310 (0.20) 308→312 (0.55) 308→313 (-0.36)	429
E3	2.981	416	0.2103	307→309 (-0.11) 308→310 (0.61) 308→312 (-0.30)	386
E4	3.039	408	0.0001	308→311 (0.69)	
E5	3.116	398	0.0001	308→314 (0.69)	
E6	3.121	397	0.1255	307→309 (-0.13) 308→310 (0.15) 308→312 (0.31) 308→313 (0.58)	360
E7	3.222	385	0.0001	308→315 (0.70)	
E8	3.269	379	0.0083	308→316 (0.69)	